The American Journal of Pathology, Vol. 184, No. 8, August 2014

ELSEVIER

The American Journal of
PATHOLOGY
ajp.amjpathol.org

CELL INJURY, REPAIR, AGING, AND APOPTOSIS

Combinatorial Therapy with Acetylation and Methylation Modifiers Attenuates Lung Vascular Hyperpermeability in Endotoxemia-Induced Mouse Inflammatory Lung Injury

Jayakumar Thangavel,* Asrar B. Malik,† Harold K. Elias,* Sheeja Rajasingh,* Andrew D. Simpson,* Premanand K. Sundivakkam,† Stephen M. Vogel,† Yu-Ting Xuan,* Buddhadeb Dawn,* and Johnson Rajasingh*‡

From the Division of Cardiovascular Diseases, Department of Internal Medicine, and the Department of Biochemistry and Molecular Biology,‡ Cardiovascular Research Institute, University of Kansas Medical Center, Kansas City, Kansas; and the Department of Pharmacology,† University of Illinois at Chicago, Chicago, Illinois*

Accepted for publication May 13, 2014.

Address correspondence to Johnson Rajasingh, Ph.D., Cardiovascular Research Institute, Department of Internal Medicine, Department of Biochemistry and Molecular Biology, University of Kansas Medical Center, Kansas City, KS 66160. E-mail: rjohnson9@kumc.edu.

Impairment of tissue fluid homeostasis and migration of inflammatory cells across the vascular endothelial barrier are crucial factors in the pathogenesis of acute lung injury (ALI). The goal for treatment of ALI is to target pathways that lead to profound dysregulation of the lung endothelial barrier. Although studies have shown that chemical epigenetic modifiers can limit lung inflammation in experimental ALI models, studies to date have not examined efficacy of a combination of DNA methyl transferase inhibitor 5-Aza 2-deoxycytidine and histone deacetylase inhibitor trichostatin A (herein referred to as Aza+TSA) after endotoxemia-induced mouse lung injury. We tested the hypothesis that treatment with Aza+TSA after lipopolysaccharide induction of ALI through epigenetic modification of lung endothelial cells prevents inflammatory lung injury. Combinatorial treatment with Aza+TSA mitigated the increased endothelial permeability response after lipopolysaccharide challenge. In addition, we observed reduced lung inflammation and lung injury. Aza+TSA also significantly reduced mortality in the ALI model. The protection was ascribed to inhibition of the eNOS-Cav1-MLC2 signaling pathway and enhanced acetylation of histone markers on the vascular endothelial-cadherin promoter. In summary, these data show for the first time the efficacy of combinatorial Aza+TSA therapy in preventing ALI in lipopolysaccharide-induced endotoxemia and raise the possibility of an essential role of DNA methyl transferase and histone deacetylase in the mechanism of ALI. *(Am J Pathol 2014, 184: 2237–2249; http://dx.doi.org/10.1016/j.ajpath.2014.05.008)*

Sepsis-induced acute lung injury (ALI) is an inflammatory disorder that affects 18 million people worldwide and 200,000 people in the United States each year[1,2] and is associated with a mortality rate of approximately 30% despite advanced interventions.[3–5] Sepsis is a primary pathogenic factor. It induces progressive respiratory failure with bilateral alveolar infiltrates and protein-rich lung edema fluid secondary to severe disruption of the lung vascular endothelial barrier.[6] Although antibiotics and volume replacement are the cornerstones of current therapy in sepsis,[7] an unchecked inflammatory response limits their effectiveness. Therapies based on a new understanding of the disease pathogenesis are needed.

DNA methylation and histone deacetylation are frequent epigenetic events that dictate gene expression and cellular fate.[8,9] We selected DNA methyl transferase inhibitor (5-Aza 2-deoxycytidine; Aza) and histone deacetylase (HDAC) inhibitor (trichostatin A; TSA) for several reasons, as follows: i) both types of inhibitors have well-established biological activities; ii) Aza is approved by the U.S. Food and Drug Administration and has the potential to be re-purposed[10,11]; and iii) both reagents have well-documented safety and side effect profiles.[12,13] We decided to use the epigenetic modifier Aza because it incorporates into DNA CpG sites opposite to a methylated CpG site, thereby inhibiting the DNA methyl

Supported in part by American Heart Association grant–Jon Holden DeHaan Foundation grant 10SDG2630181, and NIH-supported clinical and translational science award Frontiers Pilot grant (J.R.), and NIH grants R21HL97349 (J.R.) and R01 HL-117730 (B.D.).

Disclosures: None declared.

http://dx.doi.org/10.1016/j.ajpath.2014.05.008

transferase enzyme action in the DNA. This inhibition causes loss of DNA methylation in one daughter DNA strand, because DNA methyl transferase is not available to remethylate the hemi-methylated sites generated during the first round of DNA replication.[10,14] We decided to use TSA because it is a potent general inhibitor of HDACs, which chelates the center zinc finger of the HDACs, thereby inhibiting enzyme activity.[15,16] Acetylated histone is generally thought to act as an on-switch for DNA transcription. Treating cells with TSA results in acetylation of H3 and H4, thereby counteracting the tendency for nuclear compaction, and making the DNA more accessible for interaction with transcription factors.[17,18] TSA and TSA-related reagent suberoylanilide hydroxamic acid also appear to have relatively short-lived effects on histone acetylation *in vivo*,[19] suggesting that they may not cause permanent genetic changes. In humans, oral suberoylanilide hydroxamic acid induced rapid acetylation of histones in blood within 2 hours, with return to baseline within 8 hours.[19] Moreover, TSA improved survival in models of hemorrhagic shock in rodents and swine.[20] We postulated that exposure to Aza+TSA with the consequent epigenetic changes will transiently reactivate the vascular endothelial (VE)-cadherin genes that are silenced by lipopolysaccharide (LPS).

Loss of endothelial barrier plays an important role in passage of plasma proteins into lung tissue, leading to accumulation of protein-rich edema[21,22] and transmigration of neutrophils.[23,24] Studies have shown that endothelial nitric-oxide synthase (eNOS)-mediated nitric oxide (NO) production plays an important role in regulating vascular function and pathophysiology.[25] Studies have also reported that caveolin1 (Cav1), the protein associated with caveolae in endothelial cells,[26] functions as an endogenous negative regulator of eNOS activity and is held in an inactive state through direct interaction.[26–28] These findings were corroborated by our recent study showing that diminished Cav1-eNOS interaction enhanced nitration-mediated inactivation of p190RhoGAP-A, thus increasing vascular permeability.[29]

In this study, we tested the hypothesis that treatment with Aza+TSA after LPS induction of ALI through epigenetic modification of lung endothelial cells prevents inflammatory lung injury. Our studies were focused on lung endothelial cells because of their role in orchestrating lung inflammation and injury.[30,31] We showed the critical role of epigenetic modifiers Aza+TSA in preventing lung vascular hyperpermeability and ALI.

Materials and Methods

Antibodies and Reagents

We used antibodies for phospho-eNOS-Ser^{1177}, myosin light chain 2 (*MLC2*), phospho-MLC2-Thr^{18}/Ser^{19}, caspase 3 (Cell Signaling Technology, Danvers, MA), VE-cadherin, eNOS, p-eNOS, β-actin, Cav1, and p-Cav1 (Santa Cruz Biotechnology, Inc., Santa Cruz, CA) and Ly-6G6C antibody for neutrophils (Novus Biological, Littleton, CO). Secondary antibodies were horseradish peroxidase–conjugated donkey anti-mouse, anti-rabbit, and anti-goat (Santa Cruz Biotechnology, Inc.); tetramethylrhodamine isothiocyanate– and fluorescein isothiocyanate–conjugated donkey anti-mouse, anti-goat, and anti-rabbit (Jackson ImmunoResearch Laboratories, Inc., West Grove, PA), and DAPI (Life Technologies, Carlsbad, CA); antibodies eNOS, VE-cadherin, CD31 (eBioscience, San Diego, CA), and L-N^{G}-nitroarginine methyl ester (L-NAME; Calbiochem, San Diego, CA).

Mice

Male C57BL/6 mice were obtained from The Jackson Laboratory (Bar Harbor, ME). All experiments were conducted in accordance with the NIH's *Guide for the Care and Use of Laboratory Animals*[32] and were approved by the Institutional Animal Care and Use Committee of the University of Illinois at Chicago (Chicago, IL). All experiments were performed with 8- to 10-week-old mice.

Primary MLEC Culture

Primary culture of mouse lung endothelial cells (MLECs) was performed with cells immunoselected from mouse lungs as previously described.[33] Briefly, a cell suspension was prepared from lungs by digestion with 1 mg/mL collagenase II and 0.5 mg/mL dispase for 30 minutes twice, followed by filtration with 70-μm and 40-μm nylon filters. Endothelial cells were then selected with a rat antibody to mouse CD31 (Millipore, Billerica, MA) and a secondary antibody coupled to magnetic beads (Miltenyi Biotec, Bergisch Gladbach, Germany). Purified endothelial cells were plated on 0.1% gelatin-coated six-well plates for 7 days in the complete EBM-2 medium (Lonza, Basel, Switzerland). The cells were stained with CD31 surface expression for flow cytometric analysis. The mRNA expressions of CD31, VE-cadherin, and vascular cell adhesion molecule 1 (VCAM1) were measured by quantitative real-time RT-PCR (RT-qPCR). Primary cultures of MLECs at passages 4 to 10 were used for all of the experiments. The phase-contrast microscopic image was taken to show the cobblestone pattern and elongated endothelial morphology of cells identified as endothelial cells. These primary MLECs were used for all of our *in vitro* experiments.

Cell Viability and Proliferation Assays

The *in vitro* viability and proliferation of the Aza+TSA-treated primary MLECs were evaluated by Trypan blue exclusion and MTT cell proliferation assays, respectively, as described by us earlier.[34] Briefly, MLECs were cultured with different concentrations of Aza and TSA in 12-well culture plates for 48 or 72 hours (Supplemental Figure S1), cells were harvested and exposed to Trypan blue solution (final concentration 0.1%), and the number of viable (unstained) and nonviable (stained) cells was counted with a hemocytometer.

The effect of Aza+TSA on MLEC proliferation was determined by MTT assay according to the manufacturer's instructions (Cell Proliferation Assay kit; Promega, Madison, WI). Briefly, 10^4 MLECs were cultured in 96-well culture plate (200 μL per well) in Dulbecco's modified Eagle's medium that contained 10% fetal bovine serum in the presence and absence of various concentrations of Aza+TSA for 48 hours at 37°C at 5% CO_2. MTT assay results were confirmed by manual counting under the phase-contrast microscope.

Flow Cytometric Analysis

Cells from a 6-well plate were harvested and washed twice in phosphate-buffered saline (PBS), counted, and resuspended in fluorescence-activated cell sorting buffer (1% bovine serum albumin in PBS that contained 0.01% NaN_3). For flow cytometric phenotype analysis, 1×10^6 cells were initially incubated with 10% mouse serum for 20 minutes at 4°C. Subsequently, cells were incubated with the appropriately labeled primary antibodies for 1 hour. Then the cells were washed with washing buffer three times and incubated for 20 minutes with the use of an appropriate secondary antibody. All incubations were performed on ice. Appropriate isotype controls were used in all cases. Finally, the cells were washed three times with fluorescence-activated cell sorting buffer, resuspended in 0.5 mL of PBS, and analyzed by flow cytometry (FACSCalibur version 2.0; BD Biosciences, San Jose, CA) with the use of Cell Quest software. Data were analyzed with the FlowJo software version 7 (TreeStar, Ashland, OR). Primary antibodies anti-CD31 for characterization of endothelial cells and anti-caspase 3 for apoptosis were used.

RT-qPCR

LPS-induced treated cells with Aza+TSA and untreated cells and normal cells from a six-well plate were washed once in PBS and harvested for RT-qPCR analysis as described by us earlier.[34,35] Briefly, total cellular RNA was obtained for RT-qPCR analysis to determine mRNA expression of endothelial markers CD31, VE-cadherin, and VCAM1 and cytokine inflammatory markers tumor necrosis factor α (TNFα) and IL-8. RT-qPCR analysis was performed on ViiA 7 (Life Technologies) with gene-specific primers and SYBR Green Master Mix (eBioscience). Primer sequences used for the RT-qPCR analysis were as follows: *CD31* forward (5′-TCCCCGAAGCAGCACTCTT-3′) and reverse (5′-ACCGCAATGAGCCCTTTCT-3′), VE-cadherin forward (5′-GTGGATGAGCCCCCTGTCT-3′) and reverse (5′-CAGCGGTTTCTTCTCGTTTTCT-3′), *VCAM1* forward (5′-CATGGAATTCGAACCCAAACA-3′) and reverse (5′-GGCTGACCAAGACGGTTGTATC-3′), *IL8* forward (5′-TGTCCCCAAGTAACGGAGAAA-3′) and reverse (5′-TGTCAGAAGCCAGCGTTCAC-3′), and *TNFα* forward (5′-GGCTGCCCCGACTACGT-3′) and reverse (5′-AGGTTGACTTTCTCCTGGTATGAGA-3′). The relative mRNA expression of target genes was normalized to endogenous 18S control gene (Applied Biosystems, Foster City, CA). Results were expressed as fold change in expression, and values were calculated as the ratio of induced expression to control expression.

Western Blot Analysis

Immunoprecipitation and Western blot analyses of VE-cadherin, caspase 3, p-eNOS, p-Cav1, and p-MLC2 proteins were performed as described earlier.[34] Briefly, 5×10^6 primary MLECs per lane were cultured in complete Dulbecco's modified Eagle's medium in the presence and absence of 1 μg/mL LPS and immediately treated with 50 nm of Aza, 25 nmol/L TSA, or a combination of both Aza and TSA for 30 minutes for phosphorylated proteins and 24 hours for non-phosphorylated proteins at 37°C. The cells were then washed in ice-cold PBS and solubilized by gentle rocking in 100 μL of lysis buffer. Endothelial lung cell lysates or immunoprecipitates were resolved by SDS-PAGE on a 4% to 12% gradient or 10% separating gel under reducing conditions and transferred to Duralose membrane. Membranes were blocked with 5% dry milk in 10 mmol/L Tris-HCl, pH 7.5, 150 mmol/L NaCl, and 0.05% Tween 20 for 1 hour. Membranes were then incubated with the indicated primary antibody (diluted in blocking buffer) overnight. All primary antibodies were used at the dilution of 1:1000. After three washes, membranes were incubated with horseradish peroxidase–conjugated goat anti-rabbit or mouse antibody. Protein bands were detected with the enhanced chemiluminescence method.

Immunofluorescence Staining

Protein expression was evaluated by immunofluorescence staining as described earlier.[34,35] Briefly, cultured cells and lung tissue were rinsed once with PBS and fixed with 4% paraformaldehyde (Sigma-Aldrich, St. Louis, MO) in PBS for 5 minutes, then rinsed three times with PBS, permeabilized with 0.3% Triton X-100 (Sigma-Aldrich) in PBS for 3 minutes, washed twice with PBS, and incubated overnight at 4°C with primary antibodies (eNOS, VE-cadherin, caspase 3) diluted with 2% bovine serum albumin in PBS. After three washes with PBS, cells were incubated with specific secondary antibodies for 1 hour at 37°C, and cells were rinsed three times with PBS, stained with DAPI to visualize cell nuclei, rinsed three times with PBS, air dried, and mounted in Vectashield mounting medium for fluorescent imaging. All immunofluorescence staining images were captured with either a confocal or an immunofluorescence microscope.

ChIP Assay

Chromatin immunoprecipitation (ChIP) assays for the VE-cadherin promoter region in LPS-induced MLECs treated or untreated with Aza alone, TSA alone, or Aza+TSA were performed according to the manufacturer's

protocol (Millipore), also described in our recent publication.[34,35] Briefly, approximately 5×10^6 cells in two 10-cm culture plates for each sample were incubated with 1% formaldehyde diluted in culture medium for 10 minutes at 37°C. The samples were then lyzed in SDS lysis buffer that contained protease inhibitors (1 mmol/L phenylmethylsulfonyl fluoride, 1 μg/mL aprotinin, and 1 μg/mL pepstatin A). Next, the samples were sonicated on ice to shear DNA to lengths between 200 and 1000 bp and incubated with primary antibodies to acetylated histone 3 lysine (aceH3K9, aceH3K18) and dimethylated histone 3 lysine 9 (me2H3K9; Millipore) overnight at 4°C on a shaker plate. Then samples were incubated with Salmon Sperm DNA/Protein A agarose slurry for 1 hour at 4°C on a shaker plate. After four washes with washing buffers, the pelleted protein A agarose/antibody/histone complex was incubated with elution buffer (1% SDS and 0.1 mol/L $NaHCO_3$) for 15 minutes at room temperature. Then the samples were incubated with 0.2 mol/L NaCl for 4 hours at 65°C. After DNA was recovered by phenol/chloroform extraction and ethanol precipitation, PCR was performed with VE-cadherin promoter forward (5′-CACCGCAGGGCCTGCCTAT-3′) and reverse (5′-TGTCAGCCGACCGTCTTTGGA-3′) primers. Aliquots of samples before immunoprecipitation (input) were analyzed by PCR to quantify the amount of DNA present in different samples. The relative DNA levels in each sample were normalized to its input DNA levels.[34,35]

Induction of ALI

ALI was induced in C57BL/6J mice by intraperitoneal injection of a lethal dose of LPS [40 mg/kg body weight (BW)]. One hour after LPS administration, the mice received treatment with vehicle or Aza (4.4 μmol/L/kg BW) or TSA (3.3 μmol/L/kg BW) or Aza+TSA. Survival was monitored for 14 days. For histological, gene expression, and cytokine assays, the mice received a single sublethal dose of LPS (10 mg/kg BW; Sigma-Aldrich) intraperitoneally. One hour after LPS challenge, the mice were treated intraperitoneally with either 4.4 μmol/L/kg BW Aza + 3.3 μmol/L/kg BW TSA or 4.4 μmol/L/kg BW Aza alone or 3.3 μmol/L/kg BW TSA alone. Mice were euthanized, and histological changes and gene expression were evaluated in the lung tissues on day 2. To avoid sampling bias during the processing of lung tissue sections and tissue for lung endothelial cells in culture, we followed the systematic uniform random sampling method. An initial random cut was made through the lung, followed by serial parallel slices made at a constant thickness interval. The slices were flipped 90 degrees in the same direction as described earlier.[36]

Pulmonary Microvascular Permeability

Pulmonary microvascular permeability to liquid was quantified by measuring capillary filtration coefficient (K_{fc}) as previously described.[37] Briefly, mice received a single sublethal dose of LPS (10 mg/kg BW; Sigma-Aldrich) intraperitoneally. One hour after LPS challenge, the mice were treated intraperitoneally with either 4.4 μmol/L/kg Aza + 3.3 μmol/L/kg TSA or 4.4 μmol/L/kg Aza alone or 3.3 μmol/L/kg TSA alone. Mice were euthanized at 6 hours after LPS administration, and lungs were dissected free of nonpulmonary tissue, and dry weight was determined. K_{fc} (mL/minute/cm H_2O/dry g) was calculated from the slope of the recorded weight change normalized to the pressure change and to lung dry weight.

Trans-Endothelial Electrical Resistance Assay

Real-time changes in resistance of the endothelial monolayer were measured *in vitro* to assess endothelial cell hyperpermeability and adherens junction (AJ) integrity as previously described.[37] In brief, MLECs from C57/BL6 mice were grown to confluence on polycarbonate wells that contained a small gold electrode (4.9×10^4 cm^2). Before the experiment, the confluent MLEC monolayer was kept in medium that contained 1% fetal bovine serum for 2 hours. Then LPS, followed by Aza alone or TSA alone or Aza+TSA, was added in the culture at different time points, and resistance over the MLEC monolayer was monitored. The data were subsequently presented as absolute values.

Myeloperoxidase Assay

Lung tissues were homogenized in 5 mmol/L phosphate buffer and then centrifuged at 16,200 × *g* (Sorvall Legend Micro 17R centrifuge; Thermo Electron LED GmbH, Osterode, Germany) for 20 minutes at 4°C. The pellets were resuspended in PBS that contained 0.5% hexadecyl trimethylammonium bromide and were subjected to a cycle of freezing and thawing. Subsequently, the pellets were homogenized, and the homogenates were centrifuged again. The supernatants were assayed for myeloperoxidase activity by using kinetics readings for 3 minutes, and absorbance was measured at 460 nm. The results were presented as ΔOD460/minute/g lung tissue.[38]

TUNEL Assay

To assess the survival of lung cells and the effects of Aza+TSA on survival of lung tissues, we performed an apoptosis assay on lung tissue collected on day 6. Cell death was assessed with the terminal deoxynucleotidyl transferase-mediated dUTP nick-end labeling (TUNEL) kit according to the manufacturer's instructions (Roche Applied Science, Indianapolis, IN). After TUNEL assay staining, sections were examined by confocal microscopy.

Statistical Analysis

All experiments were performed at least three times. Results are presented as means ± SEM. Comparisons were performed by analysis of variance (GB-STAT version 10; Dynamic Microsystems, Silver Spring, MD) or χ^2 test for

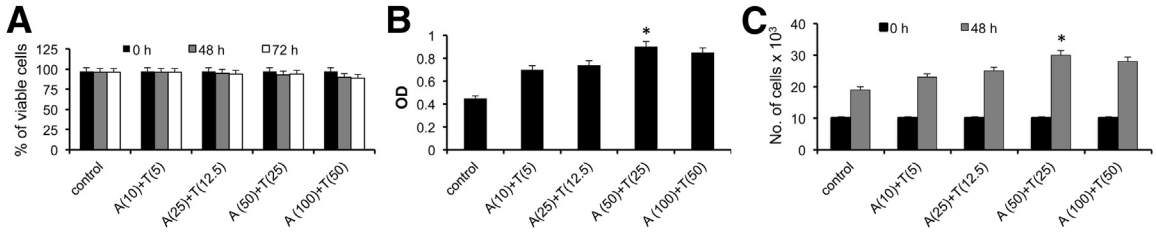

Figure 1 Assessment of Aza and TSA on lung endothelial viability and proliferation assays. Viability of MLECs after treatment with Aza and TSA as evaluated with Trypan blue dye exclusion assay. **A:** Treatment with up to 50 nmol/L Aza and 25 nmol/L TSA has no significant effect on cell viability. **B:** Proliferative effect of Aza and TSA on MLECs as determined by MTT assay. **C:** Cell proliferation by hemocytometer cell counting for 48 hours. Data are expressed as means ± SEM. $n = 3$; numbers within the parentheses indicate the concentration in nanomolar. *$P < 0.05$ versus control. A, Aza; T, TSA.

percentages. All tests were two-sided, and $P < 0.05$ was considered statistically significant. Survival between the intervention and control groups was compared with the log-rank test.

Results

Aza+TSA Treatment Does Not Affect Cell Viability

To examine toxicity of the epigenetic modifiers Aza and TSA used in this study, we performed *in vitro* viability and proliferative studies on primary MLECs. MLECs were cultured with different concentrations of Aza and TSA in 12-well culture plates for 48 or 72 hours[33] (Supplemental Figure S1), and then cells were harvested and exposed to Trypan blue solution (final concentration 0.1%), and the number of viable (unstained) and nonviable (stained) cells was counted in a hemocytometer. Treatment with up to 50 nmol/L Aza and 25 nmol/L TSA had no significant effect on cell viability (Figure 1A). Aza+TSA-treated MLECs showed normal ability to proliferate in MTT assay ($P < 0.05$) (Figure 1B). This finding was further corroborated by manual cell counting under the microscope ($P < 0.05$) (Figure 1C). Thus, our observations suggested that treatment with up to 50 nmol/L Aza and 25 nmol/L TSA had no

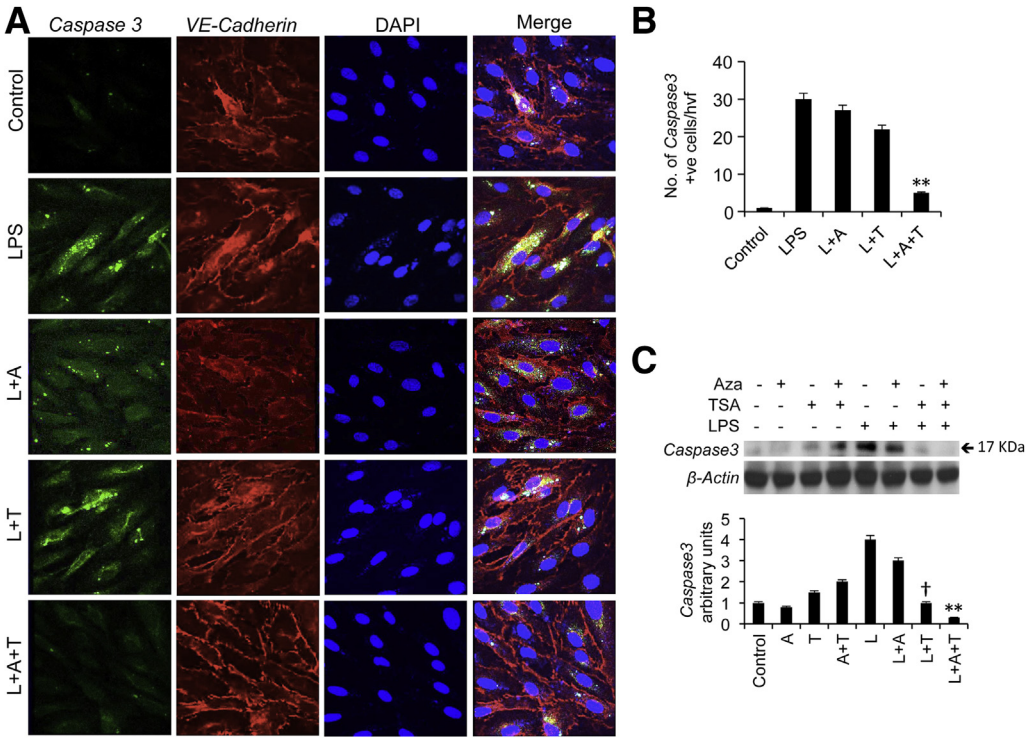

Figure 2 Aza+TSA treatment reduces lung endothelial cell apoptosis and increases cell survival after LPS exposure. **A:** Immunofluorescence staining of caspase 3 (green), VE-cadherin (red), and nuclear staining DAPI (blue). **B:** Quantification of caspase 3-positive cells shows fewer caspase 3-positive cells in LPS-induced MLECs treated with Aza+TSA compared with untreated MLECs or MLECs treated with either Aza alone or TSA alone after 24 hours of culture. **C:** Aza+TSA treatment reduces expression of cleaved caspase 3 activity. MLECs were exposed to 1 μg/mL LPS in the presence or absence of an optimal dose of 50 nmol/L Aza or 25 nmol/L TSA or Aza+TSA. After treatment for 24 hours, cells were harvested for Western blot analysis; representative Western blots for cleaved caspase 3 are shown. The combinatorial treatment with Aza+TSA inhibits the LPS-induced increase in cleaved caspase 3; β-actin was used as loading control. Protein quantification as assessed by densitometry. Data are expressed as means ± SEM. $n = 3$. **$P < 0.01$ LPS versus LPS+Aza+TSA; †$P < 0.05$ LPS versus LPS+TSA. Original magnification: ×400 (**A**). A, Aza; L, LPS; T, TSA.

toxic effect on cell viability; rather, it increased cell proliferation (Figure 1C). On the basis of these data, we further used concentrations of 50 nmol/L Aza and 25 nmol/L TSA in all of our *in vitro* experiments.

Aza+TSA Treatment Reduces LPS-Induced Endothelial Cell Apoptosis by Reducing Caspase 3 Activity and Promotes Cell Survival

Caspases are cysteine proteases, which play essential roles in apoptosis, necrosis, and inflammation. To examine whether Aza+TSA exerts anti-apoptotic actions on LPS-exposed MLECs, we performed caspase 3 staining as described by the manufacturer's instructions (Invitrogen, Eugene, OR) for flow cytometric analysis. Primary MLECs were cultured (Supplemental Figure S1) and treated with Aza+TSA in the presence and absence of 1 μg/mL LPS for 24 hours. The flow cytometric analysis showed that in the control (untreated) group, 0.6% of cells were positive for caspase 3, and the percentage of caspase 3-positive cells increased significantly to 85.3% in LPS-induced MLECs (Supplemental Figure S2, A and B). This LPS-induced increase in caspase 3 positivity was significantly reduced (64.3%) in MLECs treated with Aza+TSA compared with either Aza alone or TSA alone (85.3% versus 64.3%, respectively; $P < 0.05$) (Supplemental Figure S2, A and B). This finding was further corroborated by immunofluorescence staining for caspase 3 and VE-cadherin and by Western blot analysis for caspase 3 cleavage and activity. The immunofluorescence staining (Figure 2A) and quantitative data (Figure 2B) showed that under high-magnification visual field of the immunofluorescence microscope, 30 ± 5 cells stained positive for caspase 3 when the cells were exposed to LPS. After treatment with Aza+TSA, the number of MLECs positive for caspase 3 per high-magnification visual field decreased significantly to 5 ± 2, whereas 27 ± 4 and 22 ± 4 cells per high-magnification visual field were positive for caspase 3 in cells treated with Aza alone or TSA alone, respectively ($P < 0.01$) (Figure 2, A and B). Data from Western blot analysis further confirmed that combinatorial treatment with Aza+TSA inhibited the LPS-induced increase in caspase 3 activity ($P < 0.01$) to a greater extent compared with cells treated with either Aza or TSA alone ($P < 0.05$) (Figure 2C). Overall, these data indicated that LPS increases cleaved caspase 3 activity, committing MLECs toward apoptosis, whereas treatment with Aza+TSA reduced the increased cleaved caspase 3 activity, suggesting its role in apoptosis prevention and increased survival.

Aza+TSA Treatment Prevents LPS-Induced Lung Vascular Hyperpermeability

We quantified alterations in lung microvascular permeability by K_{fc}, as described earlier.[37] Mice were exposed to a sublethal dose of LPS (10 mg/kg BW) followed by intraperitoneal treatment with either Aza+TSA or 4.4 μmol/L/kg Aza alone or 3.3 μmol/L/kg TSA alone. In untreated mice, LPS exposure resulted in a significant increase in lung microvascular permeability compared with basal condition (Figure 3A). Strikingly, this increase in K_{fc} was significantly inhibited in mice treated with Aza+TSA (0.0587 ± 0.018 in the LPS-exposed group versus 0.029 ± 0.011 in the LPS-exposed mice treated with Aza+TSA; $P < 0.01$) (Figure 3A) rather than either alone.

To confirm our findings *in vivo* and to elucidate the mechanisms of Aza+TSA-mediated endothelial barrier protection, we studied alterations in endothelial cell junctions, crucial for the maintenance of barrier integrity. We used an *in vitro* culture system of confluent MLEC monolayer and measured trans-endothelial electrical resistance (TER), which provides an assessment of junction alterations as described earlier.[37] At 4 hours after drug treatment, all of the four groups of MLEC monolayers exhibited similar basal barrier function assessed by TER (Figure 3B). Monolayers were then challenged with 1 μg/mL LPS, and changes were monitored for 3 hours. We observed similar decreases of TER in response to LPS in all groups except the Aza+TSA-treated group ($P < 0.01$) (Figure 3B). This finding indicated that Aza+TSA treatment ameliorates LPS-induced endothelial barrier disruption. Overall, these data indicated that Aza+TSA has a protective role in

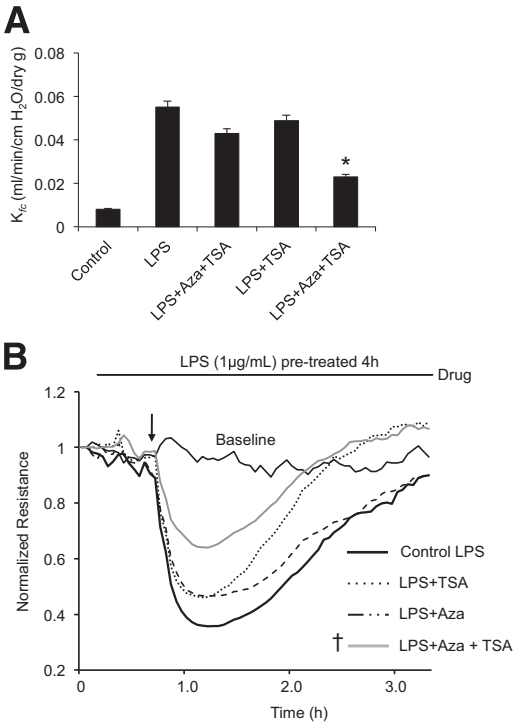

Figure 3 Treatment with Aza+TSA prevents LPS-induced lung vascular hyperpermeability determined by vascular K_{fc}. **A:** Untreated LPS-induced lungs show higher K_{fc} at 6 hours, whereas the Aza+TSA-treated lungs show significantly lower K_{fc} than the untreated LPS control lungs. **B:** TER of primary MLECs exposed to 1 μg/mL LPS for 4 hours followed by treatment with Aza+TSA or 50 nmol/L Aza alone or 25 nmol/L TSA alone for 3 hours. Data are expressed as means ± SEM (**A**). *$P < 0.05$ LPS versus LPS+Aza+TSA (**A**); †$P < 0.01$ control LPS versus LPS+Aza+TSA (**B**).

preventing lung microvascular hyperpermeability and endothelial barrier disruption in LPS-induced lung injury.

Aza+TSA in Combination Protects AJ Integrity in Endothelial Cells

To elucidate the mechanism of restoration of microvascular endothelial barrier function and AJ integrity during ALI, MLECs were cultured to confluence and stimulated with LPS, followed by treatment with either Aza+TSA or Aza alone or TSA alone for 24 hours. Next, cells were analyzed for VE-cadherin and activated eNOS protein by Western blot, RT-qPCR, and immunofluorescence analyses. With the use of confocal microscopy, we observed that, in control MLECs, VE-cadherin localized primarily at the cell borders and had a more jagged or zigzag appearance with maintenance of normal AJ integrity (Figure 4A). Neighboring cells were generally connected by interdigitating finger-like grooves, which stained positively for VE-cadherin. These structures appeared greatly exaggerated in LPS-induced MLECs. Moreover, in the AJ, VE-cadherin showed an uneven, discontinuous, or patchy pattern with small spaces in between the cell borders (Figure 4A). However, Aza+TSA-treated cells displayed cell borders with jagged or zigzag appearance and more prominent AJs similar to unstimulated control cells (Figure 4A). In addition, we observed reduced mRNA and protein expressions of VE-cadherin in MLECs exposed to LPS, which was significantly restored on treatment with a combination of Aza+TSA rather than either Aza or TSA alone ($P < 0.01$) (Figure 4, B and C). We observed an increase in the number of transcripts for VE-cadherin in LPS-challenged MLECs treated with Aza+TSA rather than the baseline control. In contrast, the VE-cadherin protein levels in the Aza+TSA-treated MLECs returned to baseline level similar to the control cells. This may be due to an increased rate of transcription but moderate level of translation in Aza+TSA-treated cells. In addition, it was not necessary that all of the transcripts be translated into protein within the observed period ($P < 0.01$) (Figure 4, B and C).

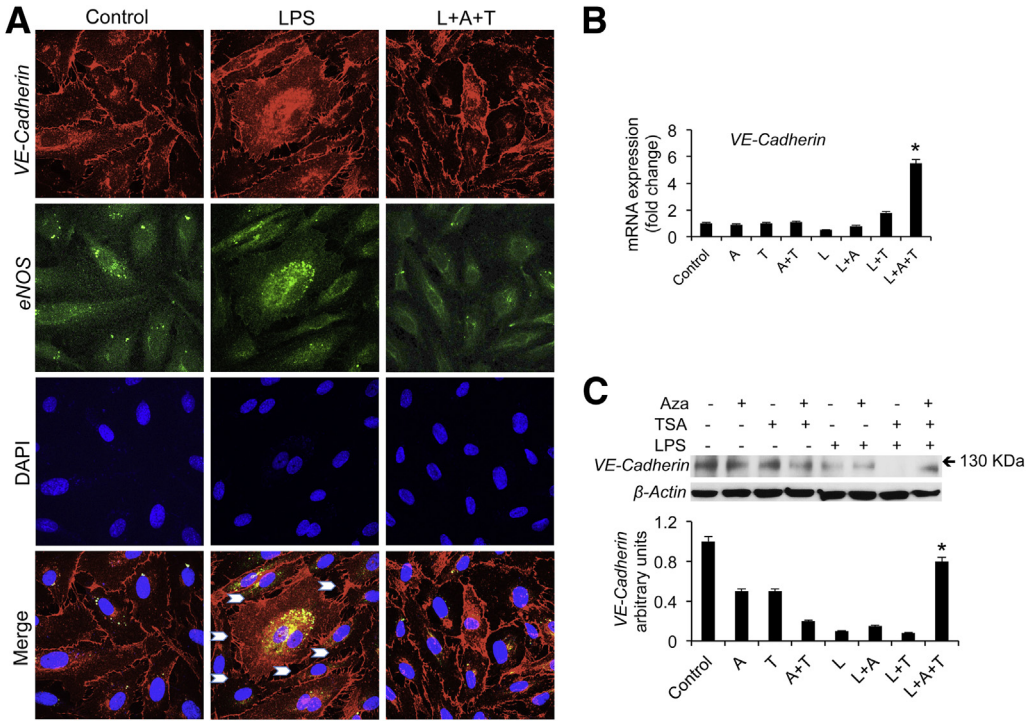

Figure 4 Treatment with Aza+TSA prevents LPS-induced loss of vascular AJ integrity. MLECs were cultured to confluence and stimulated with LPS, followed by treatment with either Aza+TSA or Aza alone or TSA alone for 24 hours. **A:** Representative confocal micrographs of TRITC-labeled VE-cadherin and FITC-labeled eNOS as detected by immunofluorescence staining. In AJ, VE-cadherin shows an uneven, discontinuous, or patchy pattern with small spaces in between the cell borders (**white arrows**). In LPS-induced MLECs, treatment with Aza+TSA restores the loss of VE-cadherin expression and displays cell borders with jagged or zigzag appearance and more prominent AJs similar to unstimulated control cells. **B:** RT-qPCR shows that the mRNA expression of VE-cadherin increases in MLECs exposed to LPS and treated with Aza+TSA than either Aza alone or TSA alone for 24 hours. Fold expression was calculated as the ratio of experimental cell expression to expression in control cells. **C:** Protein expression of VE-cadherin in MLECs exposed to LPS decreases and is significantly restored only on treatment with a combination of Aza+TSA. MLECs were cultured to confluence and stimulated with LPS, followed by treatment with optimal dosage of either Aza+TSA or 50 nmol/L Aza alone or 25 nmol/L TSA alone for 24 hours. After treatment, cells were harvested for Western blot analysis; a representative Western blot is shown. β-actin was used as a loading control. Protein quantification was assessed by densitometry ($n = 3$). The density of proteins in the control nonstimulated group was used as a standard (1 arbitrary unit) to compare the relative density of the other groups. Data are expressed as means ± SEM of three replicate experiments (**B** and **C**). *$P < 0.01$ LPS versus LPS+Aza+TSA. Original magnification: ×600 (**A**). A, Aza; FITC, fluorescein isothiocyanate; L, LPS; T, TSA; TRITC, tetramethylrhodamine isothiocyanate.

Studies have shown that stimulation of endothelial cells with LPS induces eNOS activation and nitric oxide production. Activated Cav1 is known to provide a favorable confirmation for eNOS binding and inhibition of eNOS activity and thereby maintains AJ stability.[26,28,29] Studies also indicated that Cav-1 phosphorylation enhanced binding between phospho-Cav-1 and eNOS, which was associated with a decrease in eNOS activity.[26,29] To address the significance of the eNOS-Cav1-MLC2 cascade in Aza+TSA-mediated AJ stabilization, we conducted a Western blot analysis of LPS-treated MLECs. The Western blot analysis showed an increase in levels of phosphorylated eNOS and MLC2 (Figure 5, A and C) and a decrease in phosphorylated Cav1 (Figure 5B). Both these changes were significantly reversed on treatment with Aza+TSA ($P < 0.01$) (Figure 5, A and B). To further validate the significance of the above cascade, we next inhibited eNOS by using L-NAME. We observed that the LPS-induced phosphorylation of eNOS was inhibited by the treatment with L-NAME ($P < 0.01$) (Figure 5D), whereas the treatment with Aza+TSA had no effect, further confirming that Aza+TSA acts through activated eNOS. In contrast, the phosphorylation of MLC2 did not show any reduction. This lack of reduction was probably due to the activation of MLC2 by a parallel eNOS-independent LPS-induced pathway, which was targeted by the drug treatment.[39] Future experiments are warranted to further delineate this pathway and its role in lung vascular injury. Furthermore, the reduced phosphorylation of eNOS and MLC2 by LPS-induced Aza+TSA treatment effect was blunted on treatment with L-NAME. In addition, the LPS-induced inhibition of Cav1 phosphorylation was significantly increased by treatment with Aza+TSA ($P < 0.01$), which was reduced on treatment with L-NAME (Figure 5D). This finding supports the previous study wherein L-NAME–mediated inhibition of eNOS phosphorylation resulted in reduced phospho-Cav1 levels, thereby promoting uncoupling of the eNOS/Cav1 complex and disintegration of the integrity of the endothelial junction.[26] Thus, we suggest that an Aza+TSA-dependent activated Cav1-negative feedback mechanism that returns eNOS activity to its ground state may be pathophysiologically important in vascular inflammation, which is often associated with dysregulated eNOS activity, persistent NO production, and NO modification of endothelial regulatory proteins. Together, these data indicate that Aza+TSA preserves the endothelial barrier integrity partly mediated by an eNOS-Cav1-MLC2-dependent mechanism.

Acetylation and Methylation of VE-Cadherin Promoter Region Histone 3 in LPS-Challenged Endothelial Cells Treated with Aza+TSA

Posttranslational modifications of histone N-terminal tails are dynamic and essential components in the epigenetic regulation of genes.[40] To address the posttranslational modifications of histones associated with the promoter region of VE-cadherin in restoring the microvascular endothelial barrier function and AJ integrity during ALI, MLECs were cultured to confluence and stimulated with LPS, followed by treatment with either Aza+TSA or Aza alone or TSA alone for 24 hours. The cells were then analyzed for altered acetylation and methylation signatures of histone proteins in the promoter region of VE-cadherin by using ChIP after induction of protection.[34,35] AceH3K9, aceH3K18, and me2H3K9 active proteins at the histone tail region of VE-cadherin promoter were less acetylated in LPS-induced MLECs and significantly more increased in cells treated with Aza+TSA ($P < 0.001$ versus LPS and $P < 0.01$ versus TSA) than in cells treated with either Aza alone or TSA alone ($P < 0.05$ versus LPS) (Figure 6). Further, the treatment with

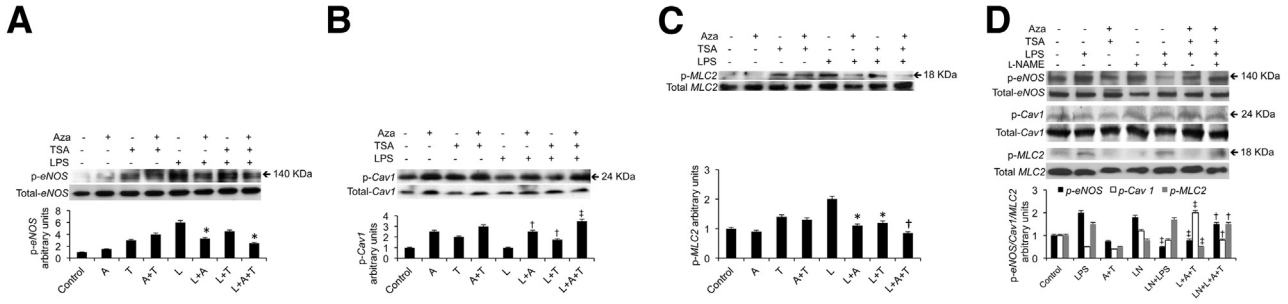

Figure 5 Aza+TSA treatment targets eNOS-Cav1-MLC2 signaling in endothelial cells. MLECs were cultured to confluence and stimulated with LPS, followed by treatment with optimal dosage of either Aza+TSA or 50 nmol/L Aza alone or 25 nmol/L TSA alone for 24 hours. After treatment, cells were harvested for Western blot analysis; representative Western blots are shown. Aza+TSA treatment reduces phospho-eNOS (Ser-1167) (**A**), increases phosphorylation of Cav1 (**B**), and reduces phosphorylation of *MLC2* in MLECs exposed to LPS and treated with Aza and TSA cultured for 30 minutes (**C**). **D:** The phosphorylation of eNOS is inhibited by the treatment with L-NAME, whereas the phosphorylation of MLC2 does not show any reduction. LPS-induced MLECs treated with Aza+TSA show reduction in phosphorylation of eNOS and MLEC2. This effect is blunted by L-NAME treatment. The LPS-induced inhibition of Cav1 phosphorylation is significantly increased by treatment with Aza+TSA. This increase is reduced on treatment with L-NAME. Total eNOS, Cav1, and total MLC2 were used as loading controls. Protein quantification was assessed by densitometry shown at the bottom of each blot. Data are expressed as means ± SEM. $n = 3$. $^{*}P < 0.05$ LPS versus LPS+Aza+TSA and LPS+Aza (**A**); $^{\dagger}P < 0.05$ LPS versus LPS+Aza and LPS+TSA, $^{\ddagger}P < 0.01$ LPS versus LPS+Aza+TSA (**B**); $^{*}P < 0.05$ versus LPS+Aza and LPS+TSA, $^{\dagger}P < 0.01$ LPS versus LPS+Aza+TSA (**C**); $^{\dagger}P < 0.05$ LPS+Aza+TSA versus LN+LPS+Aza+TSA, $^{\ddagger}P < 0.01$ LPS versus LN+LPS and LPS versus LPS+Aza+TSA (**D**). A, Aza; L, LPS; T, TSA; LN, L-NAME.

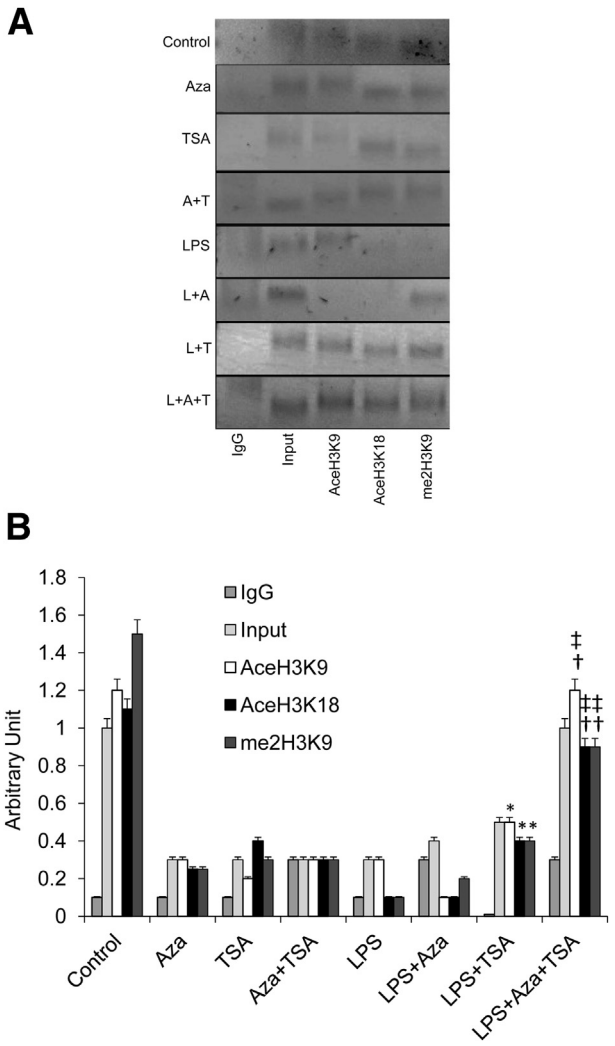

Figure 6 Epigenetic mechanism of restoring microvascular endothelial barrier function. MLECs were cultured and stimulated with LPS, followed by treatment with an optimal dose of either Aza+TSA or Aza alone or TSA alone for 24 hours. Then the cells were analyzed for altered acetylation and methylation signatures on histone proteins involved at the VE-cadherin promoter during induction of protection by ChIP with the use of antibodies of aceH3K9, aceH3K18, and me2H3K9 or anti-IgG control antibody. **A:** Acetylation and methylation status of histone H3 shows that VE-cadherin promoter is closely related to control cells and more highly acetylated and methylated in LPS-induced MLECs treated with Aza+TSA than in MLECs treated with Aza or TSA alone. **B:** Quantification of ChIP assay. Data are expressed as means ± SEM. $n = 3$. $^{*}P < 0.05$ LPS versus LPS+TSA; $^{\dagger}P < 0.01$ LPS versus LPS+Aza+TSA; $^{\ddagger}P < 0.05$ LPS+TSA versus LPS+Aza+TSA.

Aza+TSA had a significantly greater effect on the acetylation and methylation status of histone 3 than treatment with Aza or TSA alone at the VE-cadherin gene promoter in LPS-induced MLECs (Figure 6, A and B).

Aza+TSA Treatment Reduces LPS-Induced Mortality

ALI was induced in C57BL/6J mice by intraperitoneal injection of LPS (lethal dose of 40 mg/kg BW). One hour after LPS administration, mice were treated intraperitoneally either with vehicle or 4.4 μmol/L/kg BW Aza or 3.3 μmol/L/kg BW TSA or combination of Aza+TSA. Survival was monitored for 14 days, and histological changes and gene expression were evaluated in the lung at different times. All of the mice in the control group subjected to LPS died in <19 hours (0% survival), whereas mice treated with Aza died within 24 hours. The mice treated with TSA alone exhibited only a 20% survival rate, whereas mice in the Aza+TSA-treated group displayed a strikingly higher survival rate of 80% and had a prolonged survival time during the observed period of 14 days ($P < 0.01$) (Figure 7A). These data strongly support a therapeutic potential of epigenetic modifiers during endotoxemia. On day 2, immunohistochemical staining of neutrophil-specific antibody Ly-6G6C on lung tissues showed a consistently reduced LPS-induced neutrophil recruitment into the airspace after a sublethal dose of LPS in mice treated with Aza+TSA compared with mice untreated and treated with Aza alone or TSA alone (Figure 7, B and C). Lung myeloperoxidase content is a well-established indicator of

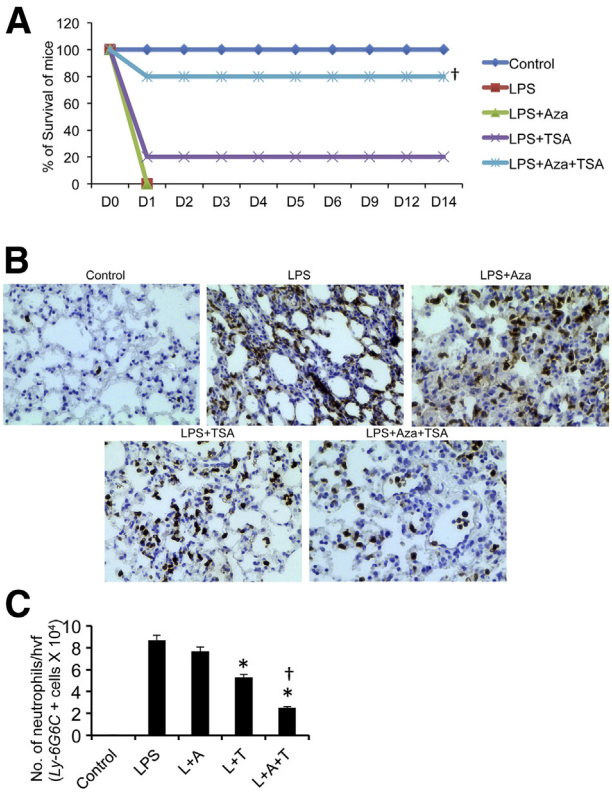

Figure 7 Aza+TSA treatment increases survival in LPS-challenged mice. **A:** Survival trend of normal mice (blue) or LPS (40 mg/kg, i.p.; red) injected mice in the presence of either no drug treatment, single modality 1 hour before therapy Aza alone (4.4 μmol/L/kg, i.p.; green), TSA alone (3.3 μmol/L/kg, i.p.; purple), or combination of Aza+TSA regimen (blue) up to 2 weeks. For histological, molecular, and immunological analyses, mice injected with 10 mg/kg LPS were treated with 4.4 μmol/L/kg Aza alone, 3.3 μmol/L/kg TSA alone, or Aza+TSA. The lung tissues and blood were collected on day 2. **B:** Representative microscopic images of lung tissue sections. **C:** The quantitative results for neutrophil infiltration. $n = 5$ (**A**; Aza alone, TSA alone, and Aza+TSA). $^{\dagger}P < 0.01$ versus LPS (**A**); $^{*}P < 0.05$ LPS versus LPS + TSA (**C**); $^{*}P < 0.05$ LPS+TSA versus LPS+Aza+TSA (**C**); $^{\dagger}P < 0.01$ LPS and LPS+Aza versus LPS+Aza+TSA (**C**). Original magnification: ×400 (**B**). A, Aza; L, LPS; T, TSA.

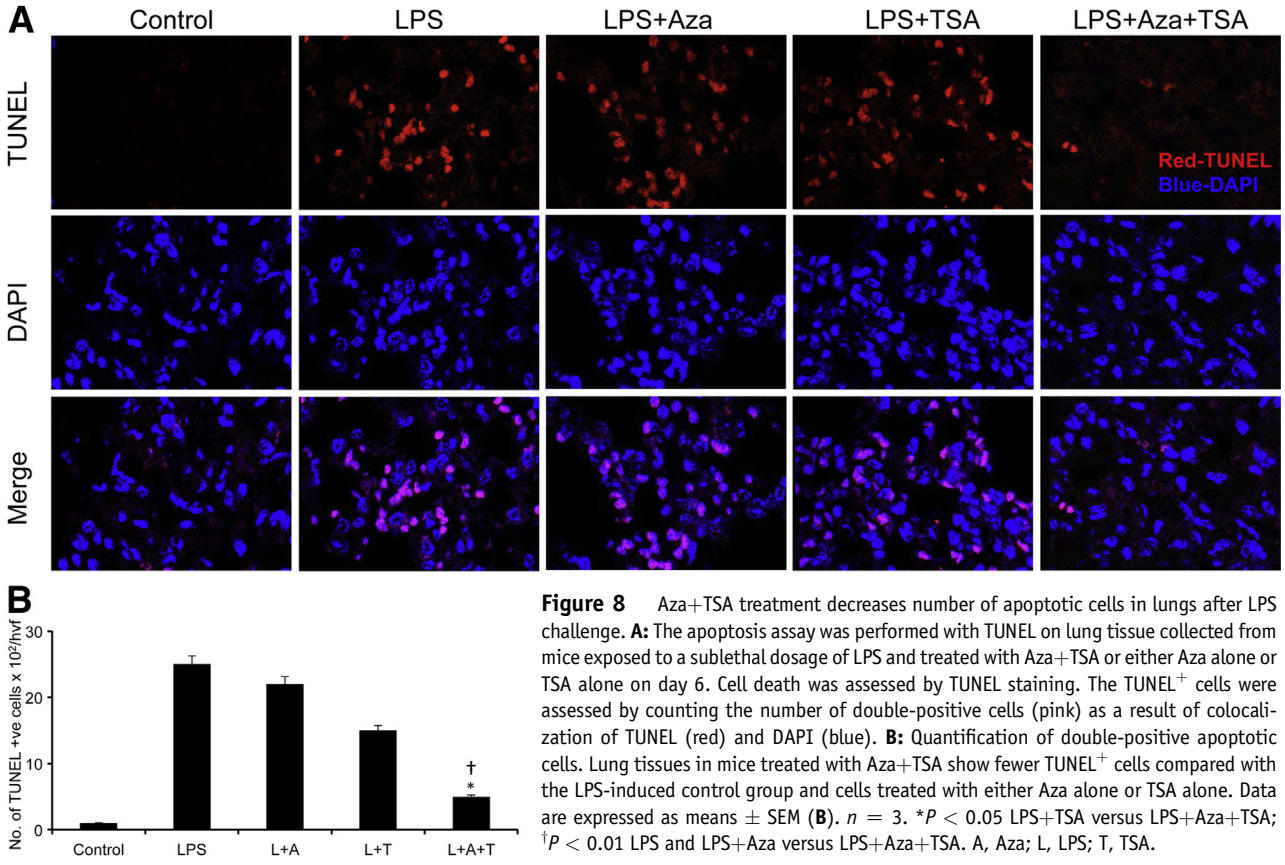

Figure 8 Aza+TSA treatment decreases number of apoptotic cells in lungs after LPS challenge. **A:** The apoptosis assay was performed with TUNEL on lung tissue collected from mice exposed to a sublethal dosage of LPS and treated with Aza+TSA or either Aza alone or TSA alone on day 6. Cell death was assessed by TUNEL staining. The TUNEL$^+$ cells were assessed by counting the number of double-positive cells (pink) as a result of colocalization of TUNEL (red) and DAPI (blue). **B:** Quantification of double-positive apoptotic cells. Lung tissues in mice treated with Aza+TSA show fewer TUNEL$^+$ cells compared with the LPS-induced control group and cells treated with either Aza alone or TSA alone. Data are expressed as means ± SEM (**B**). $n = 3$. *$P < 0.05$ LPS+TSA versus LPS+Aza+TSA; †$P < 0.01$ LPS and LPS+Aza versus LPS+Aza+TSA. A, Aza; L, LPS; T, TSA.

neutrophilic sequestration in lung injury. Myeloperoxidase content was significantly more reduced in mice treated with Aza+TSA than in untreated mice ($P < 0.01$) (Supplemental Figure S3A). We also found significantly more decreased TNFα and IL-8 gene expressions in LPS-induced lungs treated with Aza+TSA than in lungs treated with either Aza or TSA alone (TNFα, $P < 0.01$; *IL8*, $P < 0.001$) (Supplemental Figure S3, B and C).

Aza+TSA-Treated Mice Show Decreased Apoptotic Cell Numbers in Lungs

In addition, to assess apoptosis, we performed TUNEL assay staining on day 6 on the superior lobe of lung tissues from mice induced with sublethal dose of LPS and treated with Aza+TSA. We examined the sections by immunofluorescence microscopy. Cell death was assessed by colocalized double positivity of TUNEL-red and DAPI-blue (pink) (Figure 8A). The number of apoptotic cells was significantly lower in the Aza+TSA-treated group than in groups treated with either Aza alone or TSA alone ($P < 0.01$ LPS versus LPS+Aza+TSA) (Figure 8B).

Discussion

Sepsis-induced ALI is a clinical condition common in the intensive care setting, with poor outcomes for which no definitive therapies are currently available. The molecular mechanisms that regulate lung endothelial barrier repair after lung vascular injury, a primary cause of ALI from sepsis after lung injury, remain incompletely understood. This is the first study to examine the efficacy of a combinatorial treatment with epigenetic-modifying agents Aza+TSA on lung endothelial barrier function after sepsis. Our data show that treatment with a single dose of Aza+TSA in a mouse model of ALI prevented lung vascular hyperpermeability and inflammatory lung injury and promoted survival rate that compared with treatment with either Aza or TSA alone. Mechanistically, Aza+TSA treatment suppressed phosphorylation of MLC2 and eNOS and activated Cav1. The above effects are attributed to Aza+TSA-mediated epigenetic modulation of acetylated and methylated histone 3 protein of the VE-cadherin promoter.

Although epigenetic modifiers were shown to attenuate the generation of inflammatory cytokines and chemokines and inflammatory injury in the airway, digestive tract, and joints in animal models, the results have been variable.[41–44] This variability may be because previous studies examined the effects of pretreatment with HDAC inhibitors and other epigenetic modifiers rather than studying their value in therapeutic protocols. Agents such as TSA are chemotherapeutic agents that induce differentiation and promote apoptosis in transformed cells at higher concentrations.[45] TSA also suppressed the production of inflammatory cytokines in animal models of

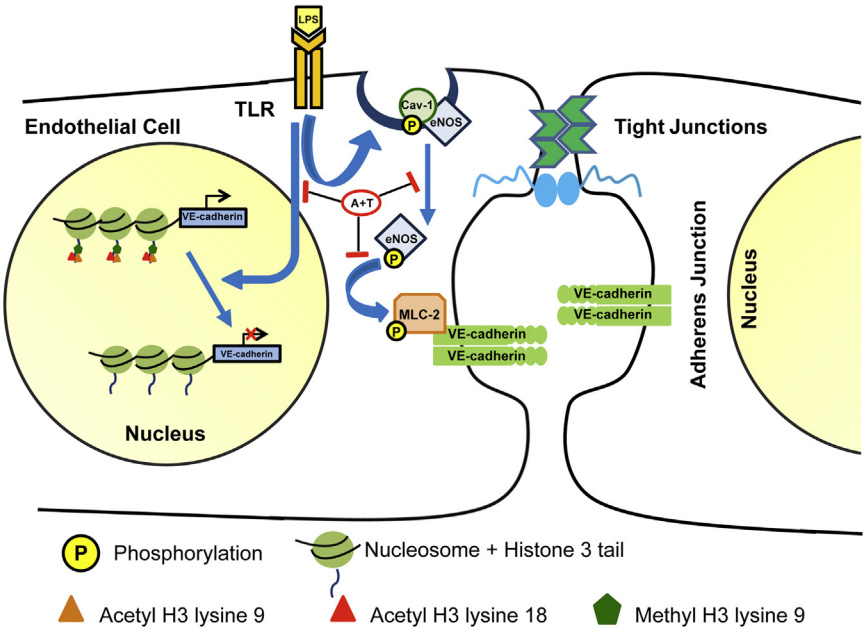

Figure 9 Schematic representation of proposed molecular mechanisms. LPS induces expression of VE-cadherin by eNOS-caveolin-MLC2 signaling mechanism in lung endothelial cells. In addition, LPS reduces acetylation and methylation of histone 3 tail (lysine residues 9 and 18) on VE-cadherin promoter. Epigenetic modifiers Aza + TSA function by inhibiting activation of eNOS-caveolin-MLC2 signaling and alterations in acetylation and methylation in VE-cadherin promoter, and thus restore the loss of integrity of AJs. A, Aza; T, TSA; TLR, Toll-like receptor.

autoimmune and inflammatory disease.[41,46,47] Our observations showed that treatment with nanomolar concentrations of Aza and TSA had no suppressive effect on cell viability; rather, both agents enhanced cell proliferation. Our data also showed that Aza+TSA treatment significantly reduced LPS-induced apoptosis of lung endothelial cells and enhanced cell survival. Studies showed that endothelial cells play a central role in pulmonary vascular hyperpermeability and consequent edema formation after inflammatory lung injury.[38] Our data indicate that combinatorial Aza+TSA therapy in nanomolar concentrations prevented these changes, and both drugs together were more efficacious than either drug alone. In this study, we used different dosages of Aza+TSA and LPS for the *in vivo* and *in vitro* experiments. In our survival study, we used a lethal dose of 40 mg/kg BW, and for all other *in vivo* experiments we used 10 mg/kg BW so that we could collect tissues from all groups of animals on day 2 and 6. We used 1 μg/mL LPS for the *in vitro* culture system, which is 1000 times less than the concentration used in the *in vivo* system. *In vitro*-based experiments are unable to withstand concentrations of the drugs used for *in vivo* studies. Hence, there is a greater likelihood of diminished cell viability and inconsistent results. Whereas, in *in vivo* experiments, despite higher drug concentrations, direct cell toxicity is limited because of the pharmacokinetics of the drug.

eNOS inhibitors prevented the increase in lung vascular permeability observed in Cav1-deficient mice, consistent with the essential role of eNOS activity and NO generation in the mechanism of increased permeability.[48] Activated (phosphorylated) eNOS in endothelial cells induced nitration of p190RhoGAP and concomitantly activated RhoA, resulting in cytoskeleton reorganization with increased contractility from increased phospho-MLC levels and retraction of VE-cadherin AJs.[29] This finding provides a causal link between eNOS and disruption of the vascular endothelial barrier.[29] Our present data show that lung endothelial cells exposed to LPS showed a significant decrease in TER, which was ameliorated by treatment with Aza+TSA. These findings were confirmed in the mouse lung experiments that showed significantly increased lung vascular filtration coefficient in LPS-exposed untreated cells, which was also significantly reduced in mice treated with Aza+TSA.

We observed a reduction in expression of VE-cadherin in lung endothelial cells exposed to LPS, which was prevented with Aza+TSA treatment. The defect in VE-cadherin was partly mediated though eNOS-Cav1-MLC2−dependent signaling, and Aza+TSA treatment seemed to function at the level of this pathway. Thus, these epigenetic modifying agents attenuated the dissociation of VE-cadherin junctions and endothelial junctional permeability.

Epigenetic modifiers produce epigenetic changes, with effects that are apparently reversible. The changes lead to modifications of DNA or chromatin, which do not involve alterations in DNA sequence.[8,49] Severe inflammation was shown to be associated with HDAC/histone acetyltransferase imbalance, which influences the acetylation status of histones in lungs and heart.[50] Here, we addressed the possibility that gene expression in endothelial cells after LPS exposure is regulated by histone modifications. Previous studies showed increased levels of dimethyl histone 3 lysine 9 and trimethyl histone 3 lysine 27 and reduced acetylation of acetylated histone 3 lysine 18 and acetylated histone 3 lysine 27, which are characteristics of heterochromatin and euchromatin, respectively.[51] We examined the status of these histone markers in the promoter region of the VE-cadherin gene. ChIP analysis showed reduced acetylation of active histone proteins aceH3K9 and aceH3K18 in VE-cadherin promoter in LPS-challenged endothelial cells, and treatment of cells with

Aza+TSA increased acetylation. Further, we observed reduced methylation of another active histone protein, me2H3K9, in VE-cadherin promoter in LPS-challenged endothelial cells, which was increased on treatment with Aza+TSA. These data suggest that the endothelial barrier protective effect of treating with combination of Aza+TSA is the result of acetylation and methylation modifications of histone at the level of VE-cadherin promoter.

Mortality studies after 14 days of follow-up found a significantly greater survival rate (80%) in Aza+TSA-treated mice than in control mice. LPS-induced infiltration of neutrophils and generation of inflammatory cytokines in lung tissues were also significantly reduced in Aza+TSA-treated mice. Mice treated with either Aza or TSA exhibited mortality similar to the untreated LPS-challenged group, with death commencing as early as within the first 24 hours of treatment. These findings further highlight the therapeutic potential of Aza+TSA.

In conclusion, a single dose of Aza+TSA administered after onset of ALI attenuated lung vascular hyperpermeability and inflammatory lung injury. The molecular mechanisms underlying the protective action of Aza+TSA involved modification of histone acetylation and methylation at the level of VE-cadherin promoter and reduced phosphorylation of eNOS and MLC2 and increased phosphorylation of Cav1 (Figure 9). Together, these observations identify a novel approach that uses epigenetic modifying agents to reverse the outcome of ALI induced by endotoxemia.

Acknowledgment

All authors contributed equally to this work.

Supplemental Data

Supplemental material for this article can be found at *http://dx.doi.org/10.1016/j.ajpath.2014.05.008*.

References

1. Nemeth K, Mayer B, Mezey E: Modulation of bone marrow stromal cell functions in infectious diseases by toll-like receptor ligands. J Mol Med (Berl) 2010, 88:5−10
2. Ware LB, Matthay MA: The acute respiratory distress syndrome. N Engl J Med 2000, 342:1334−1349
3. Price LC, McAuley DF, Marino PS, Finney SJ, Griffiths MJ, Wort SJ: Pathophysiology of pulmonary hypertension in acute lung injury. Am J Physiol Lung Cell Mol Physiol 2012, 302:L803−L815
4. Schaefer MB, Pose A, Ott J, Hecker M, Behnk A, Schulz R, Weissmann N, Gunther A, Seeger W, Mayer K: Peroxisome proliferator-activated receptor-alpha reduces inflammation and vascular leakage in a murine model of acute lung injury. Eur Respir J 2008, 32:1344−1353
5. Wheeler AP, Bernard GR: Acute lung injury and the acute respiratory distress syndrome: a clinical review. Lancet 2007, 369:1553−1564
6. Schwartz RS, Holmes DR Jr, Topol EJ: The restenosis paradigm revisited: an alternative proposal for cellular mechanisms. J Am Coll Cardiol 1992, 20:1284−1293
7. Dellinger RP, Levy MM, Carlet JM, Bion J, Parker MM, Jaeschke R, Reinhart K, Angus DC, Brun-Buisson C, Beale R, Calandra T, Dhainaut JF, Gerlach H, Harvey M, Marini JJ, Marshall J, Ranieri M, Ramsay G, Sevransky J, Thompson BT, Townsend S, Vender JS, Zimmerman JL, Vincent JL; International Surviving Sepsis Campaign Guidelines Committee; American Association of Critical-Care Nurses; American College of Chest Physicians; American College of Emergency Physicians; Canadian Critical Care Society; European Society of Clinical Microbiology and Infectious Diseases; European Society of Intensive Care Medicine; European Respiratory Society; International Sepsis Forum; Japanese Association for Acute Medicine; Japanese Society of Intensive Care Medicine; Society of Critical Care Medicine; Society of Hospital Medicine; Surgical Infection Society; World Federation of Societies of Intensive and Critical Care Medicine: Surviving Sepsis Campaign: international guidelines for management of severe sepsis and septic shock: 2008. Crit Care Med 2008, 36:296−327
8. Jenuwein T, Allis CD: Translating the histone code. Science 2001, 293:1074−1080
9. Hashimshony T, Zhang J, Keshet I, Bustin M, Cedar H: The role of DNA methylation in setting up chromatin structure during development. Nat Genet 2003, 34:187−192
10. Christman JK: 5-Azacytidine and 5-aza-2′-deoxycytidine as inhibitors of DNA methylation: mechanistic studies and their implications for cancer therapy. Oncogene 2002, 21:5483−5495
11. Wu CJ, Yang CY, Chen YH, Chen CM, Chen LC, Kuo ML: The DNA methylation inhibitor 5-azacytidine increases regulatory T cells and alleviates airway inflammation in ovalbumin-sensitized mice. Int Arch Allergy Immunol 2012, 160:356−364
12. Avila AM, Burnett BG, Taye AA, Gabanella F, Knight MA, Hartenstein P, Cizman Z, Di Prospero NA, Pellizzoni L, Fischbeck KH, Sumner CJ: Trichostatin A increases SMN expression and survival in a mouse model of spinal muscular atrophy. J Clin Invest 2007, 117:659−671
13. Kaminskas E, Farrell AT, Wang YC, Sridhara R, Pazdur R: FDA drug approval summary: azacitidine (5-azacytidine, Vidaza) for injectable suspension. Oncologist 2005, 10:176−182
14. Dhawan S, Georgia S, Tschen SI, Fan G, Bhushan A: Pancreatic beta cell identity is maintained by DNA methylation-mediated repression of Arx. Dev Cell 2011, 20:419−429
15. Furumai R, Ito A, Ogawa K, Maeda S, Saito A, Nishino N, Horinouchi S, Yoshida M: Histone deacetylase inhibitors block nuclear factor-kappaB-dependent transcription by interfering with RNA polymerase II recruitment. Cancer Sci 2011, 102:1081−1087
16. Suzuki T, Miyata N: Non-hydroxamate histone deacetylase inhibitors. Curr Med Chem 2005, 12:2867−2880
17. Qian Q, Qian H, Zhang X, Zhu W, Yan Y, Ye S, Peng X, Li W, Xu Z, Sun L, Xu W: 5-Azacytidine induces cardiac differentiation of human umbilical cord-derived mesenchymal stem cells by activating extracellular regulated kinase. Stem Cells Dev 2012, 21:67−75
18. Xu C, Police S, Rao N, Carpenter MK: Characterization and enrichment of cardiomyocytes derived from human embryonic stem cells. Circ Res 2002, 91:501−508
19. O'Connor OA, Heaney ML, Schwartz L, Richardson S, Willim R, MacGregor-Cortelli B, Curly T, Moskowitz C, Portlock C, Horwitz S, Zelenetz AD, Frankel S, Richon V, Marks P, Kelly WK: Clinical experience with intravenous and oral formulations of the novel histone deacetylase inhibitor suberoylanilide hydroxamic acid in patients with advanced hematologic malignancies. J Clin Oncol 2006, 24:166−173
20. Lin T, Chen H, Koustova E, Sailhamer EA, Li Y, Shults C, Liu B, Rhee P, Kirkpatrick J, Alam HB: Histone deacetylase as therapeutic target in a rodent model of hemorrhagic shock: effect of different resuscitation strategies on lung and liver. Surgery 2007, 141:784−794
21. Lo SK, Everitt J, Gu J, Malik AB: Tumor necrosis factor mediates experimental pulmonary edema by ICAM-1 and CD18-dependent mechanisms. J Clin Invest 1992, 89:981−988

22. Lindbom L: Regulation of vascular permeability by neutrophils in acute inflammation. Chem Immunol Allergy 2003, 83:146–166
23. Mehta D, Malik AB: Signaling mechanisms regulating endothelial permeability. Physiol Rev 2006, 86:279–367
24. Matthay MA, Wiener-Kronish JP: Intact epithelial barrier function is critical for the resolution of alveolar edema in humans. Am Rev Respir Dis 1990, 142:1250–1257
25. Atochin DN, Huang PL: Endothelial nitric oxide synthase transgenic models of endothelial dysfunction. Pflugers Arch 2010, 460:965–974
26. Chen Z, Bakhshi FR, Shajahan AN, Sharma T, Mao M, Trane A, Bernatchez P, van Nieuw Amerongen GP, Bonini MG, Skidgel RA, Malik AB, Minshall RD: Nitric oxide-dependent Src activation and resultant caveolin-1 phosphorylation promote eNOS/caveolin-1 binding and eNOS inhibition. Mol Biol Cell 2012, 23:1388–1398
27. Wunderlich C, Schober K, Lange SA, Drab M, Braun-Dullaeus RC, Kasper M, Schwencke C, Schmeisser A, Strasser RH: Disruption of caveolin-1 leads to enhanced nitrosative stress and severe systolic and diastolic heart failure. Biochem Biophys Res Commun 2006, 340: 702–708
28. Maniatis NA, Shinin V, Schraufnagel DE, Okada S, Vogel SM, Malik AB, Minshall RD: Increased pulmonary vascular resistance and defective pulmonary artery filling in caveolin-1-/- mice. Am J Physiol Lung Cell Mol Physiol 2008, 294:L865–L873
29. Siddiqui MR, Komarova YA, Vogel SM, Gao X, Bonini MG, Rajasingh J, Zhao YY, Brovkovych V, Malik AB: Caveolin-1-eNOS signaling promotes p190RhoGAP-A nitration and endothelial permeability. J Cell Biol 2011, 193:841–850
30. Abraham E, Carmody A, Shenkar R, Arcaroli J: Neutrophils as early immunologic effectors in hemorrhage- or endotoxemia-induced acute lung injury. Am J Physiol Lung Cell Mol Physiol 2000, 279: L1137–L1145
31. Song Y, Ao L, Raeburn CD, Calkins CM, Abraham E, Harken AH, Meng X: A low level of TNF-alpha mediates hemorrhage-induced acute lung injury via p55 TNF receptor. Am J Physiol Lung Cell Mol Physiol 2001, 281:L677–L684
32. Committee for the Update of the Guide for the Care and Use of Laboratory Animals; National Research Council: Guide for the Care and Use of Laboratory Animals: Eighth Edition. Washington, DC, National Academies Press, 2011
33. Zhao YY, Gao XP, Zhao YD, Mirza MK, Frey RS, Kalinichenko VV, Wang IC, Costa RH, Malik AB: Endothelial cell-restricted disruption of FoxM1 impairs endothelial repair following LPS-induced vascular injury. J Clin Invest 2006, 116:2333–2343
34. Rajasingh J, Thangavel J, Siddiqui MR, Gomes I, Gao XP, Kishore R, Malik AB: Improvement of cardiac function in mouse myocardial infarction after transplantation of epigenetically-modified bone marrow progenitor cells. PLoS One 2011, 6:e22550
35. Rajasingh J, Lambers E, Hamada H, Bord E, Thorne T, Goukassian I, Krishnamurthy P, Rosen KM, Ahluwalia D, Zhu Y, Qin G, Losordo DW, Kishore R: Cell-free embryonic stem cell extract-mediated derivation of multipotent stem cells from NIH3T3 fibroblasts for functional and anatomical ischemic tissue repair. Circ Res 2008, 102:e107–e117
36. Hsia CC, Hyde DM, Ochs M, Weibel ER; ATS/ERS Joint Task Force on Quantitative Assessment of Lung Structure: An official research policy statement of the American Thoracic Society/European Respiratory Society: standards for quantitative assessment of lung structure. Am J Respir Crit Care Med 2010, 181:394–418
37. Garcia AN, Vogel SM, Komarova YA, Malik AB: Permeability of endothelial barrier: cell culture and in vivo models. Methods Mol Biol 2011, 763:333–354
38. Di A, Kawamura T, Gao XP, Tang H, Berdyshev E, Vogel SM, Zhao YY, Sharma T, Bachmaier K, Xu J, Malik AB: A novel function of sphingosine kinase 1 suppression of JNK activity in preventing inflammation and injury. J Biol Chem 2010, 285:15848–15857
39. Shen Q, Rigor RR, Pivetti CD, Wu MH, Yuan SY: Myosin light chain kinase in microvascular endothelial barrier function. Cardiovasc Res 2010, 87:272–280
40. Cedar H, Bergman Y: Linking DNA methylation and histone modification: patterns and paradigms. Nat Rev Genet 2009, 10:295–304
41. Choi Y, Park SK, Kim HM, Kang JS, Yoon YD, Han SB, Han JW, Yang JS, Han G: Histone deacetylase inhibitor KBH-A42 inhibits cytokine production in RAW 264.7 macrophage cells and in vivo endotoxemia model. Exp Mol Med 2008, 40:574–581
42. Zhang L, Jin S, Wang C, Jiang R, Wan J: Histone deacetylase inhibitors attenuate acute lung injury during cecal ligation and puncture-induced polymicrobial sepsis. World J Surg 2010, 34: 1676–1683
43. Iwata K, Tomita K, Sano H, Fujii Y, Yamasaki A, Shimizu E: Trichostatin A, a histone deacetylase inhibitor, down-regulates interleukin-12 transcription in SV-40-transformed lung epithelial cells. Cell Immunol 2002, 218:26–33
44. Rahman I: Oxidative stress, transcription factors and chromatin remodelling in lung inflammation. Biochem Pharmacol 2002, 64: 935–942
45. Sassi FD, Caesar L, Jaeger M, Nor C, Abujamra AL, Schwartsmann G, de Farias CB, Brunetto AL, Lopez PL, Roesler R: Inhibitory activities of trichostatin A in U87 glioblastoma cells and tumorsphere-derived cells. J Mol Neurosci 2014, [Epub ahead of print], http://dx.doi.org/10.1007/s12031-014-0241-7
46. Blanchard F, Chipoy C: Histone deacetylase inhibitors: new drugs for the treatment of inflammatory diseases? Drug Discov Today 2005, 10:197–204
47. Leoni F, Fossati G, Lewis EC, Lee JK, Porro G, Pagani P, Modena D, Moras ML, Pozzi P, Reznikov LL, Siegmund B, Fantuzzi G, Dinarello CA, Mascagni P: The histone deacetylase inhibitor ITF2357 reduces production of pro-inflammatory cytokines in vitro and systemic inflammation in vivo. Mol Med 2005, 11:1–15
48. Miyawaki-Shimizu K, Predescu D, Shimizu J, Broman M, Predescu S, Malik AB: siRNA-induced caveolin-1 knockdown in mice increases lung vascular permeability via the junctional pathway. Am J Physiol Lung Cell Mol Physiol 2006, 290:L405–L413
49. Trojer P, Reinberg D: Histone lysine demethylases and their impact on epigenetics. Cell 2006, 125:213–217
50. Butt MU, Sailhamer EA, Li Y, Liu B, Shuja F, Velmahos GC, DeMoya M, King DR, Alam HB: Pharmacologic resuscitation: cell protective mechanisms of histone deacetylase inhibition in lethal hemorrhagic shock. J Surg Res 2009, 156:290–296
51. Sdek P, Zhao P, Wang Y, Huang CJ, Ko CY, Butler PC, Weiss JN, Maclellan WR: Rb and p130 control cell cycle gene silencing to maintain the postmitotic phenotype in cardiac myocytes. J Cell Biol 2011, 194:407–423